Inorganic Chemistry
Article

Inorg. Chem. **2009**, *48*, 8695–8702 **8695**
DOI: 10.1021/ic900643h

Metal-Assisted Oxazolidine/Oxazine Ring Formation in Dinuclear Zinc(II) Complexes: Synthesis, Structural Aspects, and Bioactivity

Arpita Banerjee,[†] Subhalakshmi Ganguly,[‡] Tanmay Chattopadhyay,[†] Kazi Sabnam Banu,[†] Amarendra Patra,[†] Santanu Bhattacharya,[§] Ennio Zangrando,*[,∥] and Debasis Das*[,†]

[†]*Department of Chemistry, University of Calcutta, 92 A. P. C. Road, Kolkata 700009, India,* [‡]*Chittaranjan National Cancer Institute, 37 S. P. Mukherjee Road, Kolkata 700026, India,* [§]*Department of Chemistry, Maharaja Manindra Chandra College, Kolkata 700003, India, and* [∥]*Dipartimento di Scienze Chimiche, University of Trieste, Via L. Giorgieri 1, 34127 Trieste, Italy*

Received December 17, 2008

Three novel dinuclear Zn^{II} complexes of phenol-based compartmental macrocyclic ligands have been synthesized and characterized by routine physicochemical techniques as well as by X-ray single-crystal structure analysis. The dinuclear macrocyclic complexes **1**, **2**, and **3** were obtained through a 1:2 condensation reaction of 2,6-diformyl-4-methylphenol and N-(hydroxyalkyl) ethylenediamine (L^1, L^2, and L^3, respectively) in the presence of zinc(II) acetate, followed by the addition of thiocyanate anion [L^1 = N-(2-hydroxyethyl)ethylenediamine, L^2 = N-(3-hydroxypropyl)ethylenediamine, and L^3 = N-(2-hydroxypropyl)ethylenediamine]. The synthesized 18-membered macrocycles are noted to be structurally unique, and their formation proceeds with the generation of two oxazolidine side rings in complexes **1** and **3** and two oxazine side rings in **2**, along with the creation of four new chiral centers in each case. Complexes **1** and **2** are characterized by a butterfly-like arrangement with the SCN ligands situated on the same side with respect to the Zn_2O_2 moiety, whereas the centrosymmetric complex **3** exhibits a stepped arrangement with parallel methyl-phenoxy fragments (spaced at ca. 1.5 Å) and *trans* located SCN ligands with respect to the Zn_2O_2 core. The formation of these unusual macrocycles is considered to be zinc-mediated. Preliminary studies with the complexes show that all of them exhibit an inhibitory effect, on the cell proliferation of human stomach cancer cell line AGS, though with different degrees, where complex **3** shows the highest efficiency.

Introduction

Dinuclear transition metal complexes play a central role in a variety of biological fields. It had been discovered that active sites of several metalloenzymes comprise two transition metal ions, and synthetic dinuclear receptors have been employed to mimic such active centers.[1−4] Over the past few decades, bimetallic complexes have drawn wide attention for their interesting properties arising from the close proximity of the two metal centers.[5] Zinc being an essential and one of the most bio-relevant transition metal ions, next to iron (human beings contain an average of ∼2−3 g of zinc), it is no surprise that dinuclear Zn^{II} complexes have attracted particular interest as synthetic structural mimics of the active site of a range of metalloenzymes,[6] such as zinc-dependent aminopeptidases, metallo-β-lactamases, and alkaline phosphatases.[7] The role and behavior of zinc in all such bioinorganic processes are modulated by its coordination environment, where Zn^{II} can be four-, five-, or six-coordinated. In enzymes, Zn^{II} usually has coordination numbers smaller than six, so that they have available binding sites in their coordination spheres. Substrates, in principle, can bind to zinc by the substitution of coordinated water or by

*To whom correspondence should be addressed. E-mail: dasdebasis2001@yahoo.com (D.D.).

(1) Lippard, S. J.; Berg, J. M. *Principles of Bioinorganic Chemistry*; University Science Books: Mill Valley, CA, 1994.
(2) Reedijk, J.; Bouwman, E. *Bioinorganic Catalysis*, 2nd ed.; Reedijk, J., Bouwman, E., Eds.; Dekker: New York, 1993.
(3) Karlin, K. D. *Science* **1993**, *261*, 701.
(4) Wilcox, D. E. *Chem. Rev.* **1996**, *96*, 2435.
(5) Gavrilova, A. L; Bosnich, B. *Chem. Rev.* **2004**, *104*, 349.
(6) (a) Parkin, G. *Chem. Rev.* **2004**, *104*, 699. (b) Vahrenkamp, H. *Dalton Trans.* **2007**, 4751.
(7) (a) Yamami, M.; Tanaka, M.; Sakiyama, H.; Koga, T.; Kobayashi, K.; Miyasaka, H.; Ohba, M.; Okawa, H. *J. Chem. Soc., Dalton Trans.* **1997**, 4545. (b) Sakiyama, H.; Mochizuki, R.; Sugawara, A.; Sakamoto, M.; Nishida, Y.; Yamasaki, M. *J. Chem. Soc., Dalton Trans.* **1999**, 997. (c) Kaminskaia, N. V.; Spingler, B.; Lippard, S. J. *J. Am. Chem. Soc.* **2000**, *122*, 6411. (d) Erxleben, A.; Hermann, J. *J. Chem. Soc., Dalton Trans.* **2000**, 569. (e) Abe, K.-J.; Izumi, J.; Ohba, M.; Yokoyama, T.; Okawa, H. *Bull. Chem. Soc. Jpn.* **2001**, *74*, 85. (f) Sakiyama, H.; Igarashi, Y.; Nakayama; Hossain, M. J.; Unoura, K.; Nishida, Y. *Inorg. Chim. Acta* **2003**, *351*, 256. (g) Chen, J.; Wang, X.; Zhu, Y.; Lin, J.; Yang, X.; Li, Y.; Lu, Y.; Guo, Z. *Inorg. Chem.* **2005**, *44*, 3424. (h) Jikido, R.; Shiraishi, H.; Matsufuji, K.; Ohba, M.; Furutachi, H.; Suzuki, M.; Okawa, H. *Bull. Chem. Soc. Jpn.* **2005**, *78*, 1795. (i) Sakiyama, H.; Ono, K.; Suzuki, T.; Tone, K.; Ueno, T.; Nishida, Y. *Inorg. Chem. Commun.* **2005**, *8*, 372. (j) Tamilselvi, A; Nethaji, M.; Mugesh, G. *Chem. Eur. J.* **2006**, *12*, 7797. (k) Mitiæ, N.; Smith, S. J.; Neves, A.; Guddat, L. W.; Gahan, L. R.; Schenk, G. *Chem. Rev.* **2006**, *106*, 3338.

Published on Web 08/26/2009

Scheme 1. A Chemical Drawing of All Three Macrocyclic Complexes

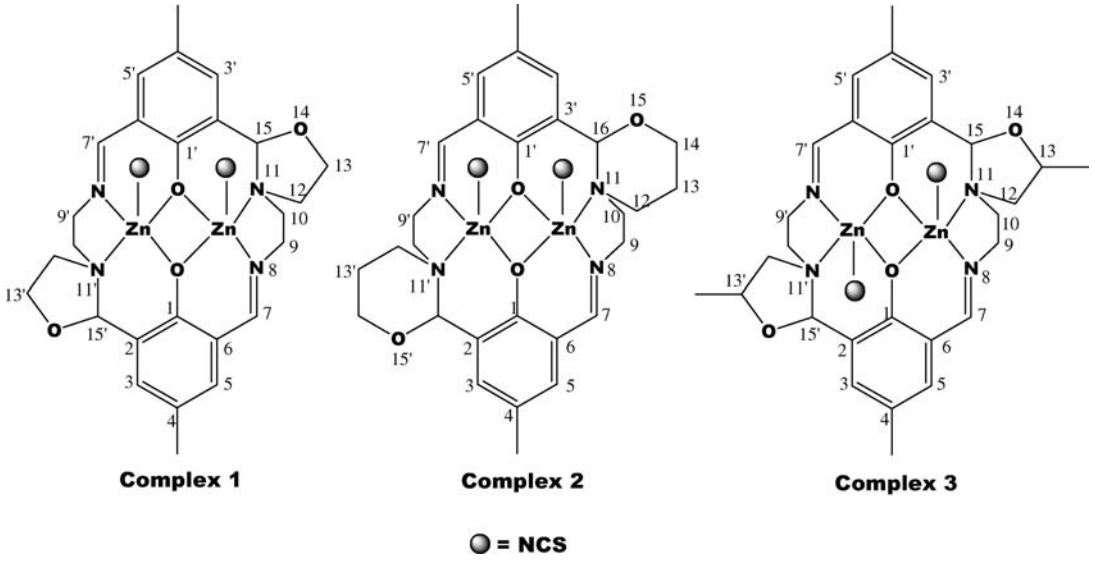

association, thus increasing the coordination number. This behavior is typical of Lewis acids, and thus zinc can act like protons in the task. Many features of zinc, such as its ability in assisting Lewis activation, nucleophile generation, fast ligand exchange, and leaving group stabilization, make Zn^{II} ideal for the catalysis of hydrolytic reactions, including DNA cleavage, which is an important property for use as anticancer drugs. DNA is generally the primary intracellular target of anticancer drugs, which cause DNA damage in the cancer cells, blocking the division of cancer cells, and resulting in cell death.[8,9] Interaction of dinuclear Zn^{II} complexes with DNA has recently attracted much attention,[10,11] owing to their possible applications as new cancer therapeutic agents and their photochemical properties, which make them potential probes of DNA structure and conformation.[12−14] With the aim to develop dinuclear Zn^{II} complexes having potential bioactivity in terms of attacking the DNA in cancer cells, we have synthesized novel dinuclear macrocyclic Zn^{II} complexes, containing two metal ions in close proximity. For this purpose, we have chosen the working elements zinc(II) acetate dihydrate, NaSCN, 2,6-diformyl-4-methylphenol, N-(2-hydroxyethyl)-ethylenediamine (L^1), N-(3-hydroxypropyl)ethylenediamine (L^2), and N-(2-hydroxypropyl)ethylenediamine (L^3) to obtain the bimetallic complexes **1**, **2**, and **3**, respectively (a chemical drawing of all three complexes is given in Scheme 1). During the reactions, macrocyclic zinc complexes showed the generation of two heterocyclic side rings, namely, oxazolidine (in the case of complexes **1** and **3**) and oxazine (in **2**), along with four new chiral centers.

Within the scope of our work, we report herein (i) the formation (metal-assisted) of unique macrocycles containing heterocyclic side rings, (ii) probable mechanistic interpretation for their generation, (iii) characterization of the dinuclear complexes, and (iv) preliminary evaluation of their *in vitro* biological effects, in terms of their anti-cancer activity on human stomach cancer cell line AGS.

Experimental Section

Physical Methods and Materials. 2,6-Diformyl-4-methylphenol was prepared according to the literature method.[15] Zinc acetate dihydrate (Sigma Aldrich), sodium thiocyanate (Merck), N-(2-hydroxyethyl)ethylenediamine (Alfa Aeser), N-(3-hydroxypropyl)ethylenediamie (TCI), and N-(2-hydroxypropyl)ethylenediamine (TCI) were purchased from commercial sources and used as received. The commercial solvents were distilled prior to complex preparation. Elemental analyses (carbon, hydrogen, and nitrogen) were performed using a PerkinElmer 240C analyzer. Infrared spectra (4000−400 cm^{-1}) were recorded at 28 °C on a Shimadzu FTIR-8400S using KBr as a medium. ^1H NMR spectra (300 MHz), ^{13}C NMR spectra (75 MHz), and two-dimensional NMR experiments (correlation spectroscopy, COSY; total correlation spectroscopy, TOCSY; rotating-frame Overhauser enhancement spectroscopy, ROESY; heteronuclear single quantum coherence, HSQC; and heteronuclear multiple-bond correlation, HMBC) were recorded in the $(CD_3)_2SO$ solvent on a Bruker AV300 Supercon NMR spectrometer using the solvent signal as the internal standard in a 5 mm BBO probe.

Cell Culture. The AGS human stomach cancer cell line was obtained from the National Center for Cell Science (NCCS), Pune, India. The cells were cultured in the F-12K (GIBCO, U.S.A.) medium, supplemented with 10% fetal bovine serum (Sigma) and 1% penicillin streptomycin (ATCC, Cat no.30−2300) in 96-well culture plates with a humidified atmosphere of 5% CO_2 in incubator (Haeraus, Germany) at 37 °C. All experiments were performed using cells from passage 15. The proliferations of the cells were assayed using a MTT cell proliferation assay kit (R&D Systems, U.S.A., Cat No. TA5355). Culture cells were treated with different concentrations of complexes **1**, **2**, and **3** (experimental groups) in contrast to control (untreated) cells.

(8) Zuber, G.; Quada, J. C., Jr.; Hecht, S. M. *J. Am. Chem. Soc.* **1998**, *120*, 9368.
(9) Hecht, S. M. *J. Nat. Prod.* **2000**, *63*, 158.
(10) Metcalfe, C.; Thomas, J. A. *Chem. Soc. Rev.* **2003**, *32*, 215.
(11) Silvestri, A.; Barone, G.; Ruisi, G.; Lo Giudice, M. T.; Tumminello, S. *J. Inorg. Biochem.* **2004**, *98*, 589.
(12) Navarro, M.; Cisneros-Fajardo, E. J.; Sierralta, A.; Fernández-Mestre, M.; Silva, P.; Arrieche, D.; Marchán, E. *J. Biol. Inorg. Chem.* **2003**, *8*, 401.
(13) Zhang, H.; Liu, C.-S.; Bu, X.-H.; Yang, M. *J. Inorg. Biochem.* **2005**, *99*, 1119.
(14) Sheng, X.; Guo, X.; Lu, X.-M.; Lu, G.-Y.; Shao, Y.; Liu, F.; Xu, Q. *Bioconjugate Chem.* **2008**, *19*, 490.
(15) Gagne, R. R.; Spiro, C. L.; Smith, T. J.; Hamann, C. A.; Thies, W. R.; Shiemeke, A. K. *J. Am. Chem. Soc.* **1981**, *103*, 4073.

Table 1. Crystallographic Data and Details of Refinements for Complexes **1**−**3**

	1	**2**·0.5H_2O	**3**
empirical formula	$C_{28}H_{30}N_6O_4S_2Zn_2$	$C_{30}H_{35}N_6O_{4.5}S_2Zn_2$	$C_{30}H_{34}N_6O_4S_2Zn_2$
fw	709.44	746.50	737.49
cryst syst	monoclinic	triclinic	triclinic
space group	$P2/n$	$P\bar{1}$	$P\bar{1}$
A (Å)	16.513(4)	9.724(3)	7.948(3)
B (Å)	9.849(3)	13.625(4)	10.216(4)
C (Å)	20.199(4)	14.787(4)	10.564(4)
α (deg)		72.41(2)	92.84(2)
β (deg)	93.31(3)	71.55(3)	108.03(3)
γ (deg)		83.43(2)	98.06(2)
volume (Å^3)	3279.6(14)	1771.2(9)	803.6(5)
Z	4	2	1
calcd density (mg/m^3)	1.437	1.400	1.524
M (Mo Kα) (mm^{-1})	1.631	1.515	1.667
F(000)	1456	770	380
θ range (deg)	1.64−26.37	1.51−26.73	2.04−25.64
collected reflns	37105	21028	11038
indep reflns	6166	7206	2845
R_{int}	0.0645	0.0371	0.0494
obsd reflns	2863	3492	1289
params	381	406	201
R_1 [$I > 2\sigma(I)$]	0.0462	0.0644	0.0441
wR_2 [$I > 2\sigma(I)$]	0.1152	0.1734	0.0916
goodness of-fit on F^2	0.829	0.928	0.747
residuals (e Å^{-3})	0.969, −0.549	0.552, −0.410	0.305, −0.284

X-Ray Data Collection and Crystal Structure Determinations. Diffraction data for the structures reported were collected at room temperature on a Nonius DIP-1030H system ($\lambda = 0.71073$ Å). Cell refinement, indexing, and scaling of the data sets were carried out using Denzo and the Scalepack suite of programs.[16] The structures were solved by direct methods and subsequent Fourier analyses[17] and refined by the full-matrix least-squares method based on F^2 with all observed reflections.[17] In the ΔFourier map of **2**, a residual was interpreted as a water molecule at half occupancy (H atoms not located). Hydrogen atoms were placed at geometrically calculated positions. All of the calculations were performed using the WinGX System, version 1.70.01.[18] Crystallographic data for all of the complexes are given in Table 1.

Syntheses. a. Complex 1. An aqueous solution of N-(2-hydroxyethyl)ethylenediamine (L^1) (2.0 equiv) was added to a solution of 2,6-diformyl-4-methylphenol (1.0 equiv) and zinc(II) acetate dihydrate (2.5 equiv) in ethanol with stirring. The reaction mixture was stirred overnight; then, solid NaSCN (4.0 equiv) was added and stirred for a further 3 h. After a few days, light yellow crystals suitable for single-crystal analysis (yield 72%) were obtained. Elem anal. found (calcd) for **1**: C, 47.50 (47.40); H, 4.22 (4.27); N, 11.71 (11.85) %. ^{1}H NMR (300 MHz, $(CD_3)_2SO$): δ 1.93 (1H, br d, 13.0 Hz, H_β-10), 2.19 (3H, s, 4-CH_3), 2.52 (1H, m, H_α-10), 3.37 (2H, m, H_α-9 and H_β-12), 3.55 (1H, m, H_α-12), 3.83 (1H, t, 13.4 Hz, H_β-9), 4.05 (2H, m, H_2-13), 5.37 (1H, s, H-15), 7.16 (1H, d, 1.9 Hz, H-5), 7.36 (1H, d, 1.9 Hz, H-3), 8.42 (1H, s, H-7). ^{13}C NMR (75 MHz, $(CD_3)_2SO$): δ 19.8 (CH_3), 47.2 (C-10), 50.2 (C-12), 53.8 (C-9), 61.7 (C-13), 91.2 (C-15) 118.8 (C-6), 124.4 (C-2), 125.0 (C-4), 132.6 (C-3), 136.7 (C-5), 159.9 (C-1), 170.5 (C-7).

b. Complex 2. Complex **2** was synthesized adopting the same procedure as for complex **1** using N-(3-hydroxypropyl)ethylenediamine (L^2) instead of L^1. After a few days, light yellow crystals suitable for single-crystal analysis (yield 68%) were obtained. Elem anal. found (calcd) for **2**: C, 48.25 (48.27); H, 4.72 (4.73); N, 11.22 (11.26) %. ^{1}H NMR (300 MHz, $(CD_3)_2SO$): δ 1.40 (1H, br d, 13.8 Hz, H_α-13), 2.15 (1H, s, 4-CH_3), 2.24 (1H, m, H_β-13), 2.25 (1H, br m, H_β-10), 3.13 (1H, br d, 11.0 Hz, H_α-10), 3.28 (1H, m, H_α-9), 3.37 (1H, m, H_α-12), 3.49 (1H, t, 12.5 Hz, H_β-12), 3.90 (1H, t, 12.6 Hz, H_β-9), 4.06 (1H, t, 11.0 Hz, H_β-14), 4.21 (1H, br dd, 11.0 Hz, 4.0 Hz, H_α-14), 5.54 (1H, s, H-16), 7.34 (1H, d, 1.9 Hz, H-3), 7.09 (1H, d, 1.9 Hz, H-5), 8.36 (1H, s, H-7). ^{13}C NMR (75 MHz, $(CD_3)_2SO$): δ 18.7 (C-13), 19.8 (CH_3), 43.5 (C-10), 47.0 (C-12), 53.1 (C-9), 68.0 (C-14), 88.4 (C-16), 118.8 (C-6), 125.0 (C-4), 126.6 (C-2), 133.9 (C-3), 137.1 (C-5), 160.0 (C-1), 171.9 (C-7).

c. Complex 3. Complex **3** was synthesized adopting the same procedure as for complex **1** using N-(2-hydroxypropyl)ethylenediamine (L^3) instead of L^1. After a few days, a light yellow crystalline solid was obtained (yield, 79%). Single crystals suitable for X-ray analysis were collected after repeated recrystallization of the crude product. Elem anal. found (calcd) for **3**: C, 48.80 (48.85); H, 4.62 (4.61); N, 11.37 (11.40) %. ^{1}H NMR (300 MHz, $(CD_3)_2SO$): δ 1.34 (1H, d, 6.1 Hz, 13-CH_3), 1.95 (1H, br t, H_α-10), 2.19 (1H, s, 4-CH_3), 2.56 (1H, m, H_β-10), 2.93 (1H, m, H_β-12), 3.36 (1H, br d, H_β-9), 3.72 (1H, m, H_α-12), 3.76 (1H, m, H_α-9), 4.49 (1H, m, 12.6 Hz, H-13), 5.53 (1H, s, H-15), 7.16 (1H, d, 1.9 Hz H-5), 7.36 (1H, d, 1.9 Hz, H-3), 8.42 (1H, s, H-7). ^{13}C NMR (75 MHz, $(CD_3)_2SO$): δ 19.7 (13-CH_3), 19.8 (4-CH_3), 47.6 (C-10), 53.5 (C-9), 57.4 (C-12), 69.2 (C-13), 89.6 (C-15), 118.8 (C-6), 124.5 (C-2), 125.0 (C-4), 132.5 (C-3), 136.6 (C-5), 160.0 (C-1), 170.4 (C-7).

Results and Discussion

Compartmental ligands with endogenous bridging phenolato moieties are of common use for modeling the active sites of metalloenzymes.[19−23] The efficiency of such ligands in the

(16) Otwinowski, Z.; Minor, W. *Processing of X-ray Diffraction Data Collected in Oscillation Mode, Methods in Enzymology*; Carter, C. W., Jr., Sweet, R. M., Eds.; Academic Press: New York, 1997; Vol. 276: Macromolecular Crystallography, part A, pp 307−326.

(17) Sheldrick, G. M. *SHELX97*, release 97-2; University of Göttingen: Göttingen, Germany, 1998.

(18) Farrugia, L. J. *J. Appl. Crystallogr.* **1999**, *32*, 837.

(19) Abe, K.-J.; Izumi, J.; Ohba, M.; Yokoyama, T.; Okawa, H. *Bull. Chem. Soc. Jpn.* **2001**, *74*, 85.

(20) Dubois, L.; Xiang, D.-F.; Tan, X.-S.; Pecaut, J.; Jones, P.; Baudron, S.; Le Pape, L.; Latour, J.-M.; Baffert, C.; Chardon-Noblat, S.; Collomb, M.-N.; Deronzier, A. *Inorg. Chem.* **2003**, *42*, 750.

(21) Williams, C. K.; Brooks, N. R.; Hillmyer, M. A.; Tolman, W. B. *Chem. Commun.* **2002**, 2132.

(22) Adams, H.; Bradshaw, D.; Fenton, D. E. *Inorg. Chim. Acta* **2002**, *332*, 195.

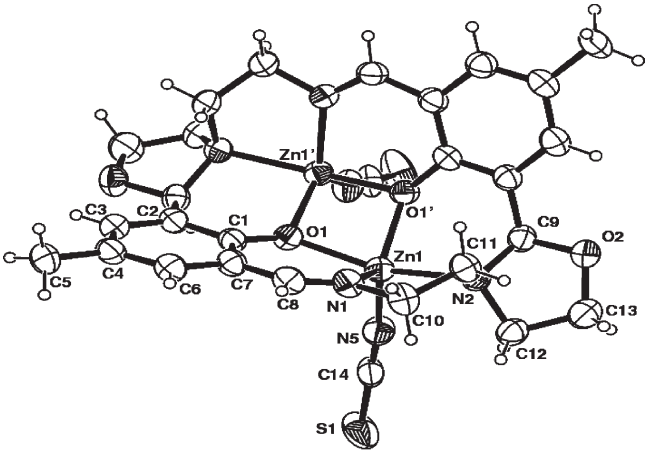

Figure 1. ORTEP drawing (30% probability ellipsoid) of molecule A of **1** arranged about a 2-fold axis.

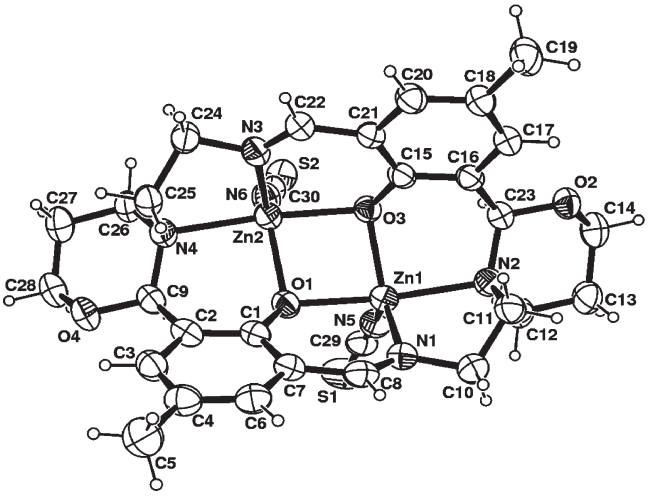

Figure 2. ORTEP drawing (30% probability ellipsoid) of **2**.

formation of dinuclear complexes and their capability of stabilizing dinuclear frameworks during reaction cycles have been well established.[24−27] Therefore, we have planned to synthesize such types of ligand complexes by adopting a template synthesis technique involving 2,6-diformyl-4-methylphenol, zinc(II) acetate dehydrate, N-(hydroxyalkyl)ethylenediamine, and sodium thiocyanate. It is important to note that, in this process, unique macrocyclic species had separated out in contrast to our expected acyclic "end-off" compartmental ligand complexes, as is evident from X-ray single-crystal analyses and NMR (^{1}H and ^{13}C) spectral study (*vide infra*).

IR data of all of the complexes show bands in the range of 1637−1643 cm^{-1} due to the presence of azomethine group and the range of 1559−1562 cm^{-1} for the skeletal vibration. A very strong band in the range of 2083−2087 cm^{-1} can be attributed to the presence of a monodentate thiocyanato ligand. However, nothing more can be said regarding the geometry of the complexes on the basis of the IR data.

Table 2. Selected Bond Lengths (Å) and Angles (deg) for **1** with esd's in Parentheses[a]

molecule A		molecule B	
Zn(1)−N(1)	2.010(4)	Zn(2)−N(3)	2.013(4)
Zn(1)−N(2)	2.170(4)	Zn(2)−N(4)	2.183(4)
Zn(1)−N(5)	1.950(5)	Zn(2)−N(6)	1.948(5)
Zn(1)−O(1)	2.075(3)	Zn(2)−O(3)	2.081(3)
Zn(1)−O(1′)	2.024(3)	Zn(2)−O(3″)	2.028(3)
Zn(1)−Zn(1′)	3.0835(13)	Zn(2)−Zn(2″)	3.0891(13)
N(1)−Zn(1)−N(2)	82.64(16)	N(3)−Zn(2)−N(4)	82.37(16)
N(1)−Zn(1)−N(5)	119.35(19)	N(3)−Zn(2)−N(6)	126.56(18)
N(1)−Zn(1)−O(1)	88.45(14)	N(3)−Zn(2)−O(3)	88.14(14)
N(1)−Zn(1)−O(1′)	120.19(15)	N(3)−Zn(2)−O(3″)	121.01(14)
N(2)−Zn(1)−N(5)	102.07(16)	N(4)−Zn(2)−N(6)	99.16(17)
N(2)−Zn(1)−O(1)	159.72(14)	N(4)−Zn(2)−O(3)	159.55(13)
N(2)−Zn(1)−O(1′)	89.01(13)	N(4)−Zn(2)−O(3″)	89.64(12)
N(5)−Zn(1)−O(1)	98.18(15)	N(6)−Zn(2)−O(3)	101.04(16)
N(5)−Zn(1)−O(1′)	120.32(18)	N(6)−Zn(2)−O(3″)	112.43(17)
O(1)−Zn(1)−O(1′)	79.77(14)	O(3)−Zn(2)−O(3″)	79.77(13)
Zn(1)−O(1)−Zn(1′)	97.59(13)	Zn(2)−O(3)−Zn(2″)	97.50(12)

[a] Symmetry codes: (′) 1/2 − *x*, *y*, 1/2 − *z*; (″) 3/2 − *x*, *y*, 1/2 − *z*.

Table 3. Selected Bond Lengths (Å) and Angles (deg) for **2** with esd's in Parentheses

Zn(1)−N(1)	2.024(4)	Zn(2)−N(3)	2.006(4)
Zn(1)−N(2)	2.235(4)	Zn(2)−N(4)	2.260(4)
Zn(1)−N(5)	1.943(5)	Zn(2)−N(6)	1.926(5)
Zn(1)−O(1)	2.119(3)	Zn(2)−O(1)	2.016(3)
Zn(1)−O(3)	2.004(3)	Zn(2)−O(3)	2.115(3)
Zn(1)−Zn(2)	3.0488(12)		
N(1)−Zn(1)−N(2)	81.62(16)	N(3)−Zn(2)−N(4)	81.89(16)
N(1)−Zn(1)−N(5)	125.16(19)	N(3)−Zn(2)−N(6)	123.6(2)
N(1)−Zn(1)−O(1)	87.81(16)	N(3)−Zn(2)−O(1)	120.36(16)
N(1)−Zn(1)−O(3)	121.27(16)	N(3)−Zn(2)−O(3)	89.40(15)
N(2)−Zn(1)−N(5)	102.61(18)	N(4)−Zn(2)−N(6)	100.84(17)
N(2)−Zn(1)−O(1)	161.08(15)	N(4)−Zn(2)−O(1)	88.88(14)
N(2)−Zn(1)−O(3)	90.09(13)	N(4)−Zn(2)−O(3)	161.87(14)
N(5)−Zn(1)−O(1)	96.31(17)	N(6)−Zn(2)−O(1)	115.99(19)
N(5)−Zn(1)−O(3)	113.44(17)	N(6)−Zn(2)−O(3)	97.23(16)
O(1)−Zn(1)−O(3)	82.00(13)	O(1)−Zn(2)−O(3)	81.82(12)
Zn(1)−O(1)−Zn(2)	94.98(13)	Zn(1)−O(3)−Zn(2)	95.47(12)

Description of Crystal Structures. Single-crystal X-ray diffraction analyses of compounds **1** and **2** showed that their geometries are very similar. The ORTEP diagrams of complexes **1** and **2** with the atom numbering scheme are depicted in Figures 1 and 2. Tables 2 and 3 represent the selected bond distances and angles for complexes **1** and **2**, respectively. In **1**, the two independent units are arranged about a crystallographic 2-fold axis, and the resultant complexes A and B slightly differ due to the orientation of their SCN groups. On the other hand, complex **2** possesses a pseudo 2-fold axis of symmetry.

The complexes are characterized by a butterfly-like arrangement (Figure 3a) with the SCN anions situated on the same side with respect to the Zn_2O_2 moiety.[28] Each Zn ion is five-coordinated and adopts a distorted trigonal bipyramidal environment, which comprises two bridging phenoxy oxygens, two N donors (from an imine and an amine group), and a NCS ligand. Thus, the two bridging phenoxy oxygens occupy an axial and an equatorial site in each metal coordination sphere. The axial Zn−O distances appear slightly

(23) Fenton, D. E. *Inorg. Chem. Commun.* **2002**, *5*, 537.
(24) Lanznaster, M.; Neves, A.; Bortoluzzi, A. J.; Szpoganicz, B.; Schwingel, E. *Inorg. Chem.* **2002**, *41*, 5641.
(25) Torelli, S.; Belle, C.; Hamman, S.; Pierre, J.-L.; Saint-Aman, E. *Inorg. Chem.* **2002**, *41*, 3983.
(26) Albedyhl, S.; Averbuch-Pouchot, M. T.; Belle, C.; Krebs, B.; Pierre, J. L.; Saint-Aman, E.; Torelli, S. *Eur. J. Inorg. Chem.* **2001**, 1457.
(27) Kaminskaia, N. V.; Spingler, B.; Lippard, S. J. *J. Am. Chem. Soc.* **2000**, *122*, 6411.
(28) Wongratchasee, W.; Chantrapromma, S.; Fun, H.-K.; Usman, A.; Karalai, C.; Ponglimanont, C.; Chantrapromma, K. *Acta Crystallogr., Sect. E* **2002**, *58*, m344.

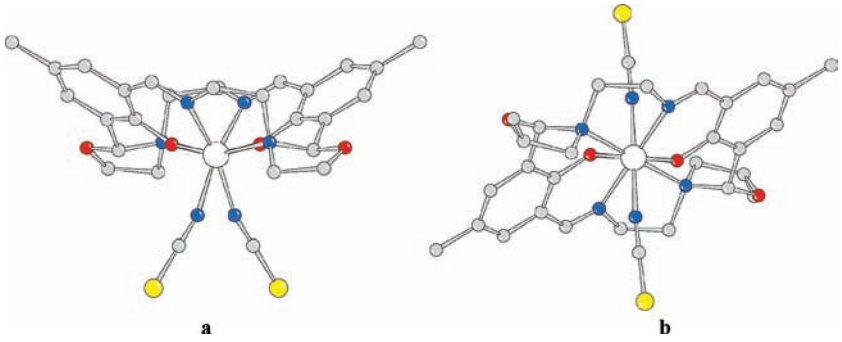

Figure 3. View of molecule A of complex **1** (a) and of molecule **3** (b) down Zn−Zn direction showing the butterfly and stepped arrangements, respectively.

Scheme 2. Plausible Mechanism for the Generation of Macrocyclic Complexes

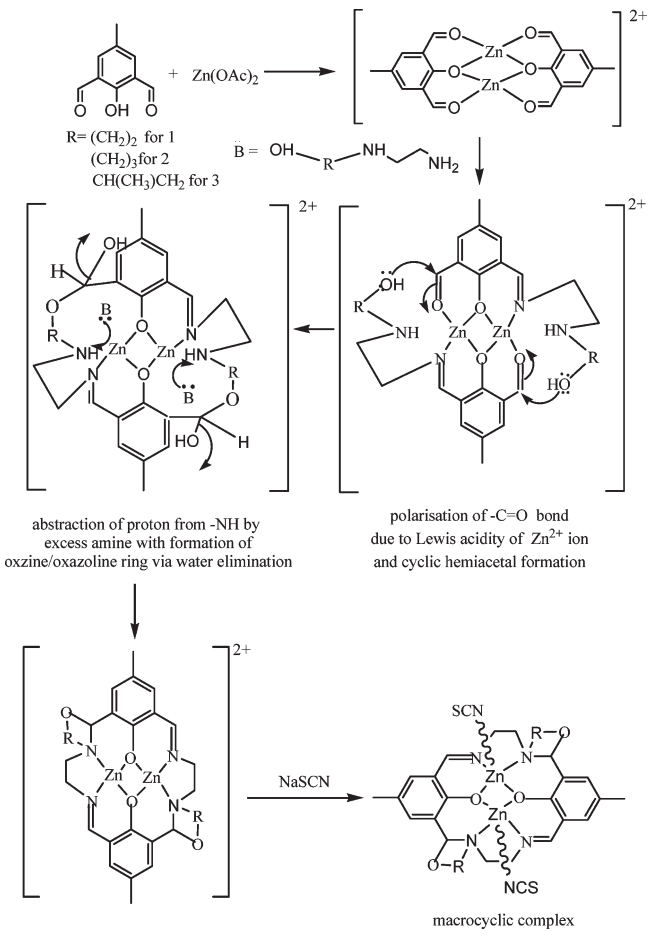

longer compared to the equatorial ones (mean values of 2.078(3) versus 2.026(3) Å in **1** and 2.118(3) versus 2.010(3) Å in **2**). All of the Zn−NCS and the Zn−N(imine) bond lengths are similar within their estimated standard deviations (esd's; range 1.926(5)−1.950(5) and 2.006(4)−2.024(4) Å in **1** and **2**, respectively). The Zn−N(amine) distances are slightly but significantly shorter in **1** (2.170(4) and 2.183(4) Å) compared to those measured in **2** (2.235(4) and 2.260(4) Å), although less strain would be expected in the metal ligation of 1,3-oxazine N in the latter. The intermetallic distances are 3.0835(13) and 3.0891(13) Å in **1** and 3.0488(12) Å in **2**, and the corresponding Zn−O−Zn bridging angles are ca. 97.5 and 95°, respectively. The Zn−Zn separation values are shorter than those usually found in Zn containing

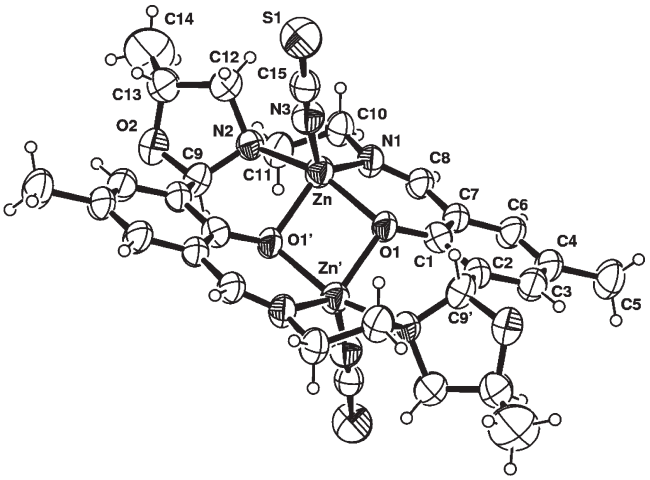

Figure 4. ORTEP drawing (30% probability ellipsoid) of **3**.

Table 4. Selected Bond Lengths (Å) and Angles (deg) for **3** with esd's in Parentheses[a]

Zn−N(1)	2.026(5)	Zn−O(1)	2.080(4)
Zn−N(2)	2.212(6)	Zn−O(1′)	2.007(4)
Zn−N(3)	1.943(7)	Zn−Zn′	3.093(2)
N(1)−Zn−N(2)	83.1(2)	N(2)−Zn−N(3)	101.5(2)
N(3)−Zn−N(1)	127.4(2)	N(2)−Zn−O(1)	156.6(2)
N(3)−Zn−O(1′)	107.8(2)	N(2)−Zn−O(1′)	85.92(19)
N(1)−Zn−O(1)	87.8(2)	N(3)−Zn−O(1)	101.1(2)
N(1)−Zn−O(1′)	124.8(2)	O(1′)−Zn−O(1)	81.65(17)

[a] Symmetry codes: (′) $-x+1, -y, -z+1$.

Robson-type[29] macrocycles (ca. 3.1 Å), to which correspond Zn−O−Zn angles larger than 98°.[30−34] The oxazine ring in **2** adopts a chair conformation, and the oxazolidine in the two complexes of **1** relieve the ring strain through a twist about the N(2)−C(9) bond. The dihedral angles formed by the methylphenoxy fragments are 81.67(7) and 73.84(7)° (in molecules A and B, respectively, of **1**) and 70.01(8)° in **2**. The presence of chiral centers N(2), N(4), C(9), and C(23) in **2** (N(2) and C(9) atoms and their symmetry related in **1**) causes the species to assume a folded rather than a planar

(29) Pilkington, N. H.; Robson, R. *Aust. J. Chem.* **1970**, *23*, 2226.
(30) Adams, H.; Bailey, N. A.; Bertrand, P.; Rodriguez de Barbarin, C. O.; Fenton, D. E.; Gou, S. *J. Chem. Soc., Dalton Trans.* **1995**, 275.
(31) Huang, W.; Gou, S.; Qian, H.; Hu, D.; Chantrapromma, S.; Fun, H. K.; Meng, Q. *Eur. J. Inorg. Chem.* **2003**, 947.
(32) Huang, W.; Chu, Z.; Gou, S.; Ogawa, T. *Polyhedron* **2007**, *26*, 1483.
(33) Atkins, A. J.; Black, D.; Finn, R. L.; Marin-Becerra, A.; Blake, A. J.; Ruiz-Ramirez, L.; Li, W.-S.; Schröder, M. *Dalton Trans.* **2003**, 1730.
(34) Huang, W.; Gou, S.; Hu, D.; Chantrapromma, S.; Fun, H.-K.; Meng, Q. *Inorg. Chem.* **2001**, *40*, 1712.

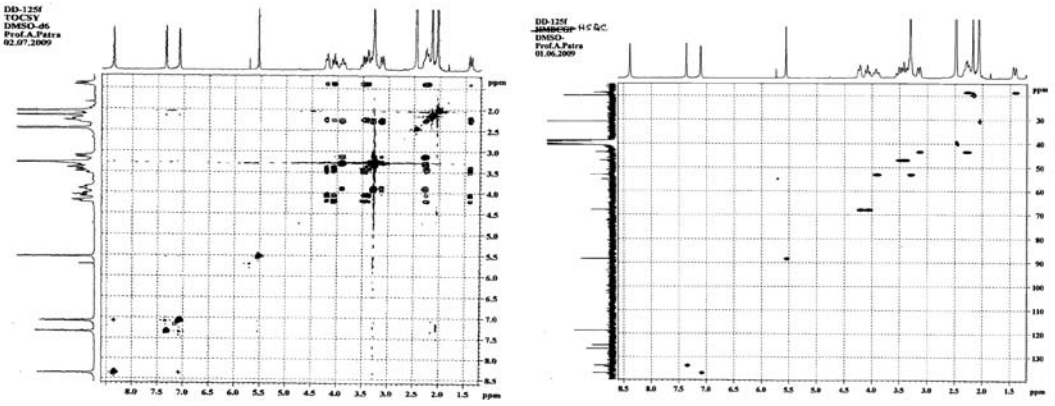

Figure 5. (a) TOCSY experiment for complex **2** and (b) HSQC experiment for complex **2**.

arrangement, as observed in many examples of these Schiff-base macrocycles.[30−34]

The use of the N-(2- hydroxypropyl)ethylenediamine (L^3) ligand, bearing a chiral center, resulted in the formation of the diastereoisomer **3**, which had been hypothesized on the basis of molecular model building. An ORTEP view of the complex with the atom labeling scheme is shown in Figure 4, and a selection of bond lengths and angles is given in Table 4. This centrosymmetric molecule exhibits a stepped arrangement (Figure 3b) with parallel methyl-phenoxy fragments (spaced at ca. 1.5 Å) and *trans*-located SCN anions with respect to the Zn_2O_2 core (Figure 4). The coordination geometry and bond lengths, as well as the intermetallic distance (3.093(2) Å), are comparable to those observed in the *cis* species, **1**, although the Zn−N(2) bond distance (2.212(6) Å) is slightly longer than those measured in **1** (2.170(4), 2.183(4) Å).

The X-ray structural characterization (see above) reveals that the complexes generated in a one-pot synthesis are structurally unique. These species differ from "classical" Robson-type[29] macrocycles. In fact, the use of N-(hydroxyalkyl)ethylenediamine in the template synthesis leads to the formation of heterocyclic side rings along with the generation of four new chiral centers (Scheme 2). It deserves special mention that all chiral centers in **1** and **2** possess the same configuration in each complex (R or S), whereas in **3** the chiralities of N(2) and C(9) are different from the symmetry-related counterpart (RR versus SS). Moreover, complexes **1**−**3** manifest a different configuration, basically with SCN ligands on the same side (*cis* isomer) or on different sides (*trans* isomer) of the phenolato planes. Complexes **1** and **2** have two N-bonded thiocyanate groups at the *cis* position and exhibit a butterfly arrangement (when viewed down Zn−Zn direction, Figure 3a). Complex **3**, on the other hand, has two thiocyanate groups located at a *trans* position and exhibits a stepped arrangement (Figure 3b).

In order to understand the structure of the complexes in solution and to ascertain their consonance with the structure derived from X-ray single-crystal structure analysis, we have performed various NMR experiments (^{1}H and ^{13}C both 1D and 2D). The NMR studies clearly indicate that complex **2** is the sole macrocyclic isomer, whereas complexes **1** and **3** are major diastereomers mixed with minor isomers (Supporting Information file). The structures of complexes **1**−**3** were corroborated by NMR studies, in which the shift assignments and spatial relationships of the various protons were established from a consideration of chemical shift theory[35] and the coupling pattern of individual ^{1}H signals in the first place and subsequent two-dimensional ^{1}H NMR shift correlations involving COSY, TOCSY, and ROESY experiments. The COSY experiment (Supporting Information file) identified the scalar coupling patterns, while the TOCSY experiment (Figure 5a) identified those protons in the same set coupling directly as well as with each of the conjugates. Thus, the methelene proton resonance of the oxazine moiety in complex **2** and those in the oxazolidine unit in complexes **1** and **3** were identified from those of the $=N-CH_2-CH_2-N<$ fragment present in each of them. The ROESY experiment (Supporting Information file) picked up ^{1}H nuclear systems having a dipolar coupling by being proximate to each other, as exemplified in Figure 6 for complex **2**.

The proton-noise decoupled one-dimensional ^{13}C NMR spectra of complexes **1**−**3** exhibited resonances typical of a C_2 or S_2 symmetric system as appropriate. The identification of the various carbon signals as $-CH_3$, $>CH_2$, $>CH-$, or $>C<$ were made from results of a DEPT-135 experiment. A subsequent HSQC experiment identified a protonated carbon signal with the resonance position of the proton directly linked (Figure 5b). This experiment also permitted identification of the resonance position for diastereomeric methylene protons. Thus, the methylene carbons of the oxazolidine ring could be sorted out from the rest, that is, those of the $=N-CH_2-CH_2-$ portion. Identification of the nonprotonated carbon resonances rested on the HMBC experiment (Supporting Information file). Here, correlations are noted for the ^{1}H signal with the signal of carbons which are usually two or three bonds apart. Thus in **2** CH_3 protons displayed long-range correlations with the quaternary C-4 carbon (resonating at δ125.0) to which it is linked along with protonated aromatic carbon resonances at δ 137.1 (C-3) and 133.9 (C-5). Proton H-8 exhibited long-range correlation with nonprotonated resonances at δ 118.8 (C-6) and 160.0 (C-1) as also with the methylene carbon resonance at δ 53.1 (C-9). The methine

(35) Silverstein, R. M.; Webster, F. X. *Spectrometric Identification of Organic Compounds*, 6th ed.; John Wiley: New York, 1998.

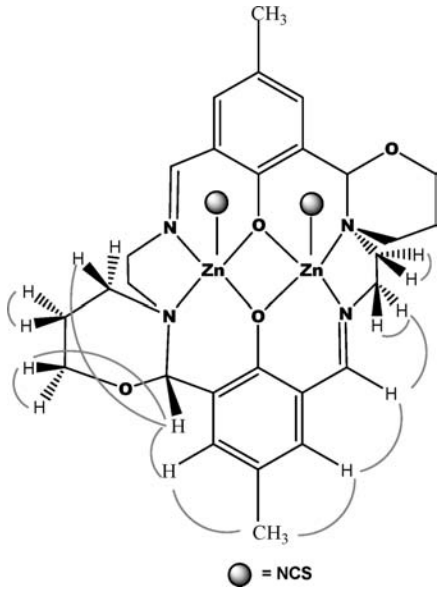

Figure 6. ROESY correlation in complex **2**.

proton singlet resonance at δ 5.54 (H-16) displayed correlation signals for nonprotonated carbon signals at δ 126.6 and 160.0 and in consonance with their association with C-2 and C-1, respectively. The result of the HMBC studies for complex **2** is shown in the Supporting Information as an illustrative example. The resonance assignments for the complex **1** and complex **3** were achieved similarly and also by their mutual ^{1}H and ^{13}C chemical shift comparison with those of **2**.

The synthesis of macrocyclic Schiff bases where macrocyclation leads to internal ring formation is a relatively new reaction, and only a few examples are published formerly.[36] Finally, it is worth noting that all attempts to synthesize the pure macrocyclic ligands in the absence of zinc(II) were unsuccessful. The same reaction scheme, performed by using different metal ions, namely, Ni^{II}, Cu^{II}, and Mn^{II}, have failed to isolate any macrocyclic product, whereas with nickel, we got "end-off" compartmental ligand complexes with L^2 (the result will be published elsewhere; the Supporting Information file contains the ORTEP view of the complex). These data confirm beyond a doubt that the formation of these Zn^{II} macrocycles is actually a metal-assisted process. The formation of these rare macrocyclic complexes can be rationalized by considering the mechanism as depicted in Scheme 2.

Bio-Activity. The three synthesized complexes were tested as possible therapeutic agents in terms of their anticancer property *in vitro*. The biological activities of all three complexes were evaluated *in vitro* on the growth kinetics of human stomach cancer cell line AGS at a concentration from 25 nM to 150 μM. This range was chosen because nonspecific tumor cell membrane damage was apparent above 150 μM (as evident from the results of a trypan blue dye exclusion test), and below 25 nM each compound failed to elicit any biological effect. Irrespective of their chemical structure, all of the complexes showed significant AGS cell growth inhibition at different concentrations. However, the degree of inhibition showed some differences among the complexes. Figure 7 represents the effect of complex **3** (as a representative) on AGS cell proliferation *in vitro*. For all compounds, the highest degree of inhibition was observed at a complex concentration of 125 μM, where complex **3** showed 66.3% inhibition of tumor cell proliferation (50.8% for **1** and 40.9% for **2** in the Supporting Information file) compared to the control. Following treatment, the inhibition of stomach cancer cell proliferation is proportional to the increases of the concentration of the respective complex in cell culture from 25 nM to 125 μM. However, the exposure of cells at a complex concentration of 150 μM showed a little decrease of tumor cell growth inhibition for all species **1**, **2**, and **3**.

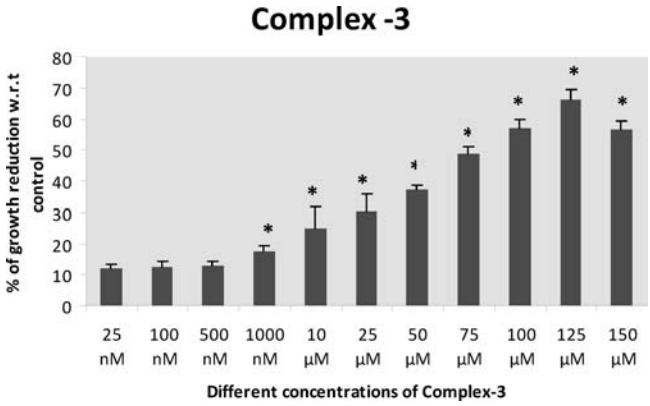

Figure 7. The effect of complex **3** on AGS cell proliferation *in vitro*. Cells were incubated with different concentrations of the complex for 48 h. The number of proliferating cells was determined through MTT assay and is presented as a percent of control cell proliferation (untreated). Results are the means $\pm$ the standard error of three separate experiments performed in triplicate wells. $^{*}P < 0.05$ when compared with the control.

In brief, the preliminary evaluation of biological activity of these complexes showed considerable tumor cell proliferation inhibition action, and among them, complex **3** appears to possess the highest anticancer activity. However, from these results, nothing conclusive can be said about the molecular mechanisms by which these complexes elicited their anticancer activity on human stomach cancer cells, AGS. On the basis of these *in vitro* studies, detailed animal experimentation might reveal further insight into the biological activity of these compounds in tumor-bearing hosts and will help to generate clinically relevant information for developing possible new anticancer drugs.

Conclusion

For the first time, it has been noticed that, in the presence of zinc(II), the condensation reaction between 2,6-diformyl-4-methylphenol and N-(hydroxyalkyl)ethylenediamine does not produce any "end-off" compartmental ligand as could be expected, but rather, a very unique cyclization process takes place with the generation of an 18-membered macrocyle having oxazolidine (in complexes **1** and **3**) or oxazine (in **2**) side rings. This cyclization is most probably zinc-mediated, as the presence of other metal ions individually failed to isolate any macrocycle of similar configuration.

(36) (a) Drew, M.; Nelson, J.; Nelson, S. M. *J. Chem. Soc., Dalton Trans.* **1981**, 1678. (b) Adams, H.; Bailey, N. A.; Fenton, D. E.; Good, R. J.; Moody, R.; Rodriguez de Barbarin, C. O. *J. Chem. Soc., Dalton Trans.* **1987**, 207. (c) Menif, R.; Martell, A. E.; Squattirito, P. J.; Clearfield, A. *Inorg. Chem.* **1990**, *29*, 4723.

The Lewis acidity of zinc(II) is supposed to be the main property that is responsible for such a distinct reaction mechanism. In addition to the unique structural features of complexes **1**, **2**, and **3**, preliminary *in vitro* studies of these dinuclear zinc(II) complexes on human stomach cancer cells, AGS, show that all of them have definite potency to inhibit tumor cell proliferation, and complex **3** appears to be the most promising in this action. To the best of our knowledge, there is no report on the use of these kinds of ligands/complexes as cytotoxic agents. On the basis of the above *in vitro* studies, research is in progress to unveil the molecular mechanisms by which these complexes elicit their biological activity in our laboratories. Moreover, detailed animal experimentation on the reported complexes will help to generate clinically relevant information for developing possible new anticancer drugs.

Acknowledgment. We gratefully acknowledge Dr. P. S. Das Gupta of Chittaranjan National Cancer Institute, Kolkata for MTT cell proliferation assay. A.B. is grateful to CSIR, India (Award No.09/028(0681)/2006-EMR-I, Dated: 07/03/2007) for financial support.

Note Added after ASAP Publication. This article was published ASAP on August 26, 2009, with minor text errors in the Experimental Section and an incorrect version of Scheme 1. The correct version was published ASAP on September 14, 2009.

Supporting Information Available: X-ray crystallographic data in CIF format of complexes **1**−**3** and additional figures. This material is available free of charge via the Internet at http://pubs.acs.org.